HIGH-RESOLUTION ONE-DIMENSIONAL MODELING OF A GAS TURBINE COMBUSTOR USING EULERIAN-LAGRANGIAN METHOD

R. Khodadadi*, N. Zamani Meymian*, H. Rashidzadeh, J. Houshmand*** and H. Khaledi*****

*Department of Mechanical Engineering, Tarbiat Modares University, Tehran, Iran
**Department of Mechanical Engineering, Islamic Azad University, Tabriz Branch, Tabriz, Iran
***Turbotec Co., Institute of Science and Technology, Sharif University of Technology, Tehran, Iran

Abstract

In this paper, a dynamic combustor model for inclusion into a one-dimensional full gas turbine engine simulation model, with high numerical accuracy is developed. Effects of dominant parameters, such as frequency and amplitude of the inlet air and fuel mas flow rate fluctuations, on outlet temperature of the combustion chamber, are investigated. The main goal of this research is to analyze the response of the gas turbine combustor to dynamic events that occur in the compressor. In the present work, for modeling combustion, the equations of chemical equilibrium (a second-law concept) are developed and applied to combustion-product mixtures. Thus the heat released from combustion is computed and used as a source term in the energy equation. Ignition effects either would be considered with a time lag equation as a source term in the energy equation. The combustor flammability limits are determined by using available experimental data for various gases and also Le Chatelier's law. Source terms of governing equations are added using the operator splitting method. To operate this, the modified version of the PPM algorithm called PPMLR is used which solves the Euler equations in Lagrangian coordinates. At the end of each time step, results calculated in the Lagrangian coordinates would remap to the original Eulerian coordinate. The results revealed that to achieve a grid-independent solution, the accuracy of 0.002 m over the length of the combustion chamber should be applied. By reducing the accuracy of simulation, numerical diffusion causes a rise in flow temperature along with the combustion chamber. Through the dynamic modeling aspect, it is found that by increasing inlet fuel flow rate frequency up to 25 Hz, the amplitude of the fluctuations of outlet temperature, increases. Further increase in frequency up to 100 Hz, the amplitude of the fluctuations remains unchanged. However further increases in frequency from 100 Hz, causes amplitudes of outlet temperature fluctuations to decrease.

Introduction

The combustor supplies an environment in the gas turbine engine in which stable and efficient combustion happens. The primary zone in the combustor provides a near-stoichiometric region of recirculating flow which provides the incoming fuel and air mixture adequate time to react and burn. All of the air flow exiting the compressor is not used in the primary zone combustion process. Some percentage of the air flows surrounding the internal liner and is mixed with the hot combustion products downstream of the primary zone [1]. Due to the intrinsic dynamics of the fluid system, the transient performance of a gas turbine engine can differ significantly from that predicted from quasi-steady operating assumptions. The outcome of these dynamics can be quite dramatic, including the unexpected crossing of the compressor surge line while transitioning between operating points. Beyond the surge line, compressor rotating stall and surge serve as the forcing functions for a complex dynamic interaction between the engine components. These unsteady operating cycles are of particular interest, as they result in considerably reduced performance and durability. Since it is impossible to guarantee that an engine can avoid such behavior during its operational lifetime, recovery from rotating stall and surge is an important issue facing the gas turbine designer. Because of this, significant efforts have been made to accurately simulate the performance of a compressor undergoing a surge transient [2]. As these techniques have developed, the focus increasingly has shifted toward extending these methods to surround the entire engine, and, thus, capture the important compressor-combustor interactions that occur during engine surge [3]. One of the more challenging tasks in this effort is the combustor behavior modeling. In the earliest days of gas turbine engine development, combustor design was regarded as black art, typically involving labor-intensive parametric testing. As the "art" evolved into more of a science, rule-based design techniques relying on experimental correlations became an important part of the initial design phase [4]. More recently, as the industry was challenged by ever more stringent requirements for performance and emissions, advanced computational modeling has played an important role in the design sequence. Ideally, a combustor model would address the actual physical processes, including the effects of three-dimensional, turbulent, viscous reacting flow. Unfortunately, such models require vast computational resources that ban their use as a design tool. As a result, numerous efforts have been made over the past 35 years to produce simplified models to predict gas turbine combustor performance [4]. These models and numerical techniques have primarily focused on the simulation of steady flow in combustors, with particular emphasis in the past 20 years on engine [5]. Similar models have been completed for other components of gas turbines prior to the combustor such as the axial compressor [6] and the diffuser [7]. Considering the modeling difficulties experienced in a steady flow, it is not surprising that little effort has been directed on addressing the added complexity of the transient behavior of the combustor. To capture the effect of the combustor on system stability, further refinements of this model introduced a set of control volumes representing the combustor geometry [8]. The heat released from the reaction was evenly distributed throughout the entire combustor section, with the presence of a flame-based upon fixed equivalence ratio criterion. Similar to the approach taken for the compressor model, an ignition delay was imposed which lagged the heat release during re-light with a time constant taken from experimental measurements, analogous to the treatment of the turbomachinery terms that were included. Aerodynamic Turbine Engine Code (ATEC) results are presented by Garrard [3]. This type of model has demonstrated its effectiveness in characterizing the dynamics of the gas turbine, albeit with certain limitations. One of these limitations is the accuracy with which the model can characterize the combustor behavior. The simple quasi-steady heat release formulation employed in the model has limited ability to accurately predict heat release, flame-out, re-light, and fuel migration in the combustor. Despite these limitations, the current models have shed new light on the importance of the compressor-combustor interaction during the engine surge event. Costura [9] developed a dynamic combustor model for a one-dimensional full gas turbine engine simulation code. A flux-difference splitting algorithm was used to numerically integrate the quasi-one-dimensional Euler equations, coupled with species mass conservation equations. The combustion model involves a single-step, global finite-rate chemistry scheme [9].

The main goal of this research is to analyze the response of the gas turbine combustor to dynamic events that occur in the compressor. For example, when the compressor surge phenomenon occurs, causes the air flow to the combustion chamber are reduced. The overall cross-sectional area of the combustion chamber is specified for the geometry. Because of the one dimensional formulation of the model, the liner of the combustion chamber is neglected [3].

Governing equations

In this section the governing equations of compressible flow are presenting firstly and then, the energy equation relations, calculation of heat release, combustion delay time and applying the numerical algorithm to the model are discussed. The unsteady one-dimensional Euler equations, supplemented with the combustion source term in energy equation and also the source term due to cross-section area variation presented in both energy and momentum equations are numerically integrated using a first-order finite difference techniques. These equations, have written in conservative Eulerian form below [10].

$$\frac{\partial \rho}{\partial t}+\nabla.\left(\rho u\right)=0 \tag{1}$$

$$\frac{\partial \rho u}{\partial t}+\nabla.\left(\rho uu\right)+\nabla p=\rho F \tag{2}$$

$$\frac{\partial \rho \varepsilon}{\partial t}+\nabla.\left(\rho \varepsilon u\right)+\nabla\left(pu\right)=G+\rho u.F \tag{3}$$

$$P=\rho RT \tag{4}$$

Equations 1 to 4 are continuity, momentum, energy, and equation of state of an ideal gas. ε is the total specific energy, ρ is the mass density, p the pressure, and F and G are momentum and energy source terms.

Combustion modeling

In the present work, the equation of chemical equilibrium is applied for combustion modeling in the combustor. Thus the heat released of combustion would be computed and used as a source term of the energy equation. The amount of heat released depends on five primary variables. The equivalence ratio, the combustion efficiency, the flammability limits, and the LHV (low heating value) [3]. The combustor flammability limits are determined by using experimental data, available for various gases [11]. These experimental data are presented just for a single fuel composition, thus for computing the mixture flammability, this model uses Le Chatelier's law. Le Chatelier arrived at his mixture rule for lower flammability limit of the gas mixture from his experiments with methane and other lower hydrocarbons [12]. The proposed empirical mixing rule is expressed as Eq. (5),

$$LFL_{mix}=\frac{1}{\sum_{i=1}^{N}\frac{y_i}{LFL_i}} \tag{5}$$

where, y_i is the mole fraction of the i^{th} component considering only the combustible species, and LFL_i is the lower flammability limit of the i^{th} component in volume percent, LFL_{mix} is the lower flammability limit of the gas mixtures. Algebraically, Le Chetelier's method states that the mixture flammability limit has a value between the maximum and minimum of the pure component flammability limits. In addition, Kondo et al. have shown that Le Chatelier's Law can be extended to UFL (upper flammability limit) estimation for some blended fuels with acceptable accuracy [12]. That is,

$$UFL_{mix}=\frac{1}{\sum_{i=1}^{N}\frac{y_i}{UFL_i}} \tag{6}$$

In order for stable combustion to occur, the primary zone equivalence ratio (φ_{pz}) must fall within a rich limit (φ_R) and a lean limit (φ_L):

$$\varphi_L \leq \varphi_{pz} \leq \varphi_R \quad (7)$$

During the dynamic operation of the combustor, it is possible for the combustion process (and hence the heat release) to occur for a short period of time even though the combustor equivalence ratio may lie outside the steady-state flammability limits. Likewise, the combustion process may not resume immediately after the combustor equivalence ratio reenters the flammability bounds due to ignition time delays. To account for these effects, Davis proposed using a first-order lag on the heat release rate similar to the one used in the compressor model which is incorporated in the present combustor model as [13]:

$$\tau_{comb}\frac{dQ_x}{dt} + Q_x = (Q_x)_{ss} \quad (8)$$

where, Q_x is the heat release rate in the control volume as is used in the governing equations (Equation (3)), $(Q_x)_{ss}$ is the steady-state value of the heat release rate calculated in the combustor model at the current time step, and τ_{comb} is a time constant used to model the combustor heat release response time. Time constants are provided to lag both the flame extinction process and the ignition process. A typical value of both time constants is 0.005 seconds. The use of the first-order time lag functions provides a model to account for such variables as radiation losses, finite chemical reaction times, and fuel diffusion effects. During reversed flow operation, it is assumed that the combustion process is extinguished, and the steady-state value of heat release would be zero.

Numerical method

The model's algorithm is based on the description of the piece-wise parabolic method (PPM) given in Colella and Woodward [10]. The numerical algorithm here is written as a Lagrangian hydrodynamics code coupled with a remap onto the original Eulerian grid. This implementation of PPM is referred to as PPMLR. The following is an outline of the PPMLR algorithm. The equations of ideal gas hydrodynamics in Lagrangian coordinates written in the conservative form are:

$$\partial_t V - \partial_m u = 0 \quad (9)$$
$$\partial_t u - \partial_m p = 0 \quad (10)$$
$$\partial_t \varepsilon - \partial_m up = 0 \quad (11)$$

where, V, u, p, and ε are the specific volume, velocity, pressure, and total energy of the gas respectively. ∂_t is the partial derivative with respect to time, and ∂_m is the partial derivative with respect to the mass coordinate. The gas density ρ and internal energy e are related to these quantities via the relations

$$\rho = 1/V,\ e = \varepsilon - 0.5u^2,\ p = (\gamma-1)\,\rho e \quad (12)$$

Here γ, the ratio of specific heats is assumed to be a constant greater than 1. The spatial coordinate r is related to the mass coordinate m via

$$m(r) = \int_{r_0}^{r} \rho(r) r dr \quad (13)$$

The function $r(m,t)$ satisfies the ordinary differential equation $dr/dt=u(m,t)$.The conservation equations can be finite differenced readily from Lagrangian equations as:

$$r_{j+1/2}^{n+1} = r_{j+1/2}^{n} + \Delta t \bar{u}_{j+1/2} \tag{14}$$

$$u_j^{n+1} = u_j^n + \frac{\Delta t}{\Delta m_j}\left(\bar{p}_{j-1/2} - \bar{p}_{j+1/2}\right) \tag{15}$$

$$\varepsilon_j^{n+1} = \varepsilon_j^n + \frac{\Delta t}{\Delta m_j}\left(\bar{u}_{j-1/2}\bar{p}_{j-1/2} - \bar{u}_{j+1/2}\bar{p}_{j+1/2}\right) \tag{16}$$

where the subscript j refers to zone-averaged values, the subscripts j-1/2 and j +1/2 refer to values at the left and right-hand interfaces of the zone, and the superscript is the time step. The variables $\bar{u}$ and $\bar{p}$ are the time-averaged values of the velocity and pressure at the Lagrangian zone interfaces [14]. In this method, every two adjacent cells, considered as a tiny shock tube problem and solved to obtain the interface average velocity and pressure. Finally, the fluid variables are instantaneously remapped from the Lagrangian coordinate system to the stationary Eulerian grid. This remap step is used the same quadratic interpolation method that is applied in the hydrodynamics step.

Validation

To validate the one-dimensional dynamic model which, is presented for gas turbine combustor, the sod's shock tube problem is solved, and the analytical solution of this problem is compared to the numerical results, that is solved with the present model.

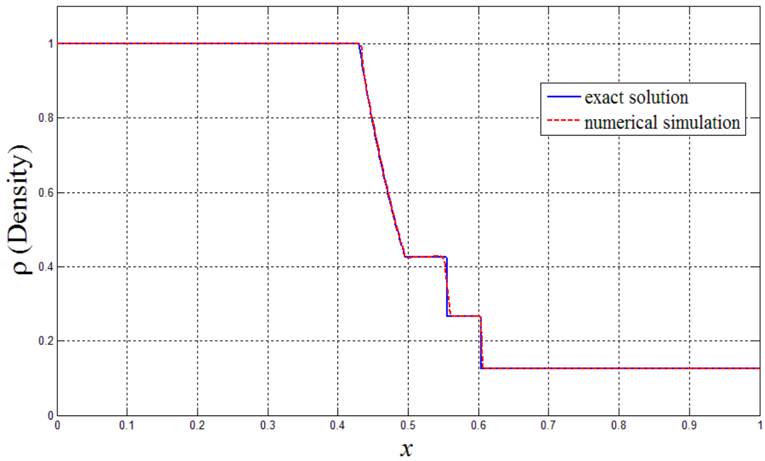

Figure 1. Density distribution along shock tube length in the time of t=2.25×10^{-4} sec, Δx=0.01.

According to figure 1 it is observed that the results of numerical models have excellent agreement with the analytical solution even in the presence of shock waves (range, 0.5 to 0.6 of the length of the tube), which is a great gradient in that area, and the behavior of the numerical model is close to the analytical solution. Therefore, this agreement declares the accuracy of the present model for modeling each unsteady compressible problem, such as modeling the gas turbine combustor.

Comparison with the analytical solution

An analytical solution [15] of a constant area combustor is used for the validation study. In figure 2, the schematic of the analytical solution is presented.

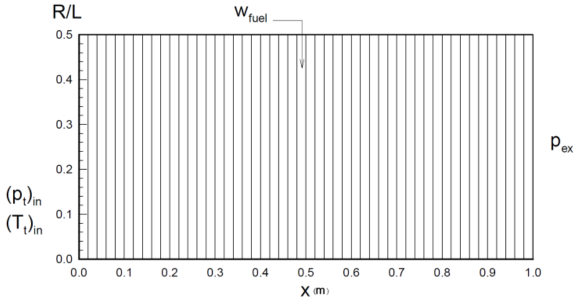

Figure 2. Schematic of constant area configuration for an analytical solution [15].

Propane (C_3H_8) is used as fuel. Total pressure loss is determined to Dpt/pt=0.0005 [16]. The length of the combustor is L=1 m. Table 1 shows the boundary condition of this study.

Table 1. Boundary and operating condition of the analytical solution.

inlet	P_i=1000 kpa, T_i=700 k, m_f=0.5 kg/s, φ=0.94, V_i=0
outlet	P_i=996.5 kpa, $\partial V_i/\partial x=0$

For additional validation, the steady-state and unsteady solution of this problem [1], is compared with the present model. In the following, the results would be discussed.

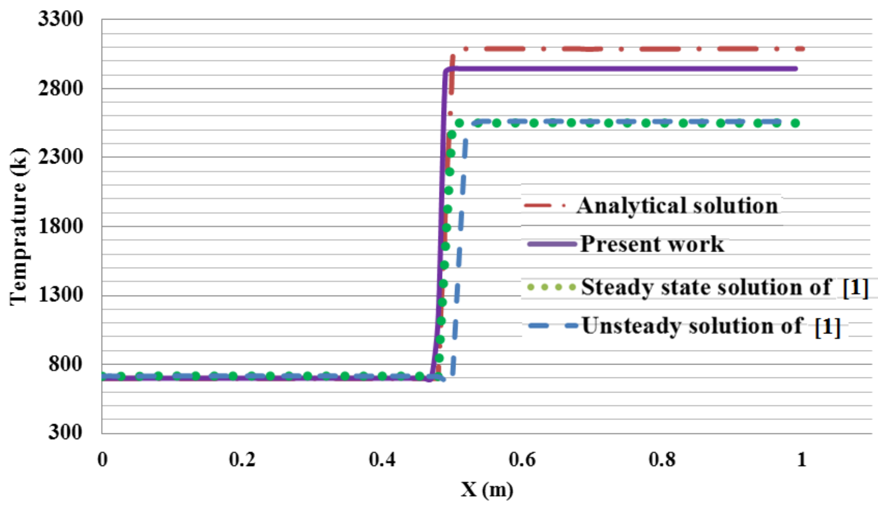

Figure 3. Comparison of the temperature distribution of present work (solid line), analytical solution (dotted dashed line) [15], steady-state solution (dotted line) [1]and unsteady solution (dashed line) [1].

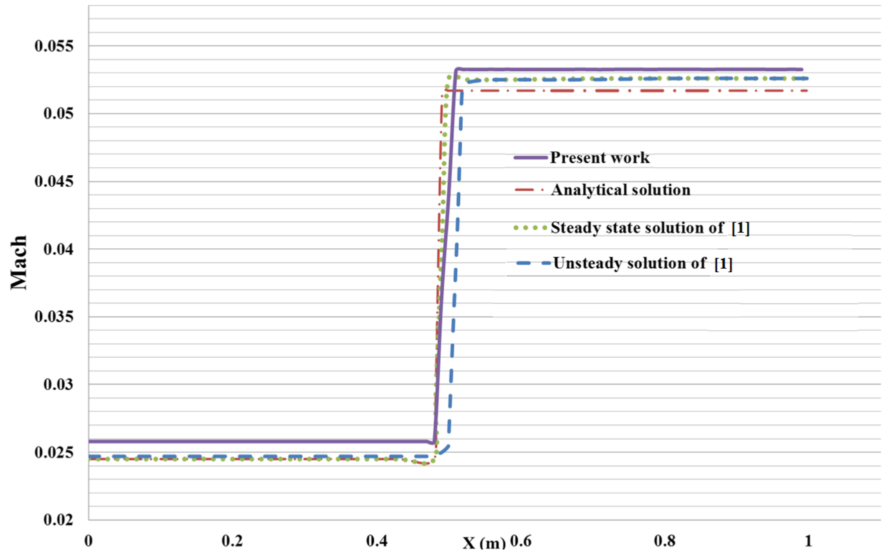

Figure 4. Comparison of Mach number distribution of present work (solid line), analytical solution (dotted dashed line) [15], steady-state solution (dotted line) [1]and unsteady solution (dashed line) [1].

The domain is discretized in 100 CVs for the numerical simulation. The total pressure loss is uniformly distributed among the CVs. The analytical solution corresponds to a steady-state compressible, calorically-perfect flow with friction. The resulting equations for this flow are derived in Hill and Peterson [15]. Figures 3 and 4 show the results for the present study. The analytical solution is compared with the present dynamic model. Also, the results are compared with a steady infinite rate and unsteady finite rate solution of Rodriguez [1]. Figure 3 presents the distribution of total temperature along the combustor. The analytical solution (essentially the first law with constant specific heats) predicts a much higher temperature than either method; this can be attributed to the calorically-perfect assumption. The unsteady solution exhibits a spatial delay before the temperature rise. This is due to the finite rate effect and the assumption that fuel enters at 300 K, i.e., a lower temperature than the inlet flow. Figure 3 illustrates that the result of the present model is much closer to the analytical solution, in contrast to Rodriguez's [1] results. The Mach number distribution is shown in figure 4. In both cases, all solutions are very close to each other. In brief, this simple case point to the fact that the results provided by the present method at the very least satisfy a necessary condition, i.e., the ability to model a textbook case often used to produce preliminary information in heat release environments [15].

Results

In this section, the effect of dynamic inputs to the gas turbine combustor performance would be discussed. The initial and boundary conditions and so the combustor entrance fuel and air flow rate, are in accordance with table 1 and table 2. Methane has been considered for the entrance fuel and chemical reactions assumed to be complete (equation (17)) and equivalence ratio is φ=0.33.

Table 2. Initial and boundary condition.

Inlet x=0	P=11.622 bar, T=651.819 k, V=0
Outlet x=L	P=11.015 bar, $\partial V/\partial x$=0
Initial condition	

P=11.622 bar, T=651.819 k, V=0
$\dot{m}_{aircte} = 59.81\ kg/\sec$, $\dot{m}_{fuel_{cte}} = 1.178\ kg/\sec$

$$CH_4 + (0.2095O_2 + 0.780869N_2 + 0.0093AR + 0.0003CO_2) \rightarrow YO_{2C} + YN_{2C} + YAR_C + YCO_{2C} + YH_{2C} \tag{17}$$

Simulation time and time step are considered t=0.15 sec and dt=2.5×10^{-06}, respectively. Also, the combustion time lag is considered τ_{comb}=0.001 sec. Combustion chamber length is L=1 m and flame domain began from X=0.3 m to X=0.665 m (flame length is obtained from 3D steady-state CFD simulation). The combustor entrance fuel flow rate is varied by time according to the equation $\dot{m}_{fuel} = A \times \sin(\omega t) + \dot{m}_{f_{cte}}$, where A is the amplitude variation of fuel flow rate and is equal to 0.59 and the mean fuel flow rate is $\dot{m}_{f_{cte}} = 1.179 \text{Kg/sec}$. Also, the fluctuation of frequency is considered ω=1000 Hz. Therefore the entrance fuel flow rate would be as figure 5.

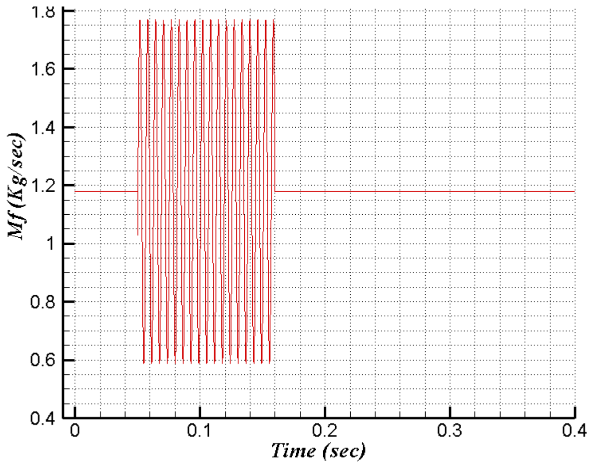

Figure 5. Inlet combustor fuel flow rate distribution.

According to figure 5, it is observed that in the time between 0.5 to 0.15 seconds, a dynamic input is entered into the system. Consequent fluctuations in heat release in the combustion chamber is shown in figure 6.

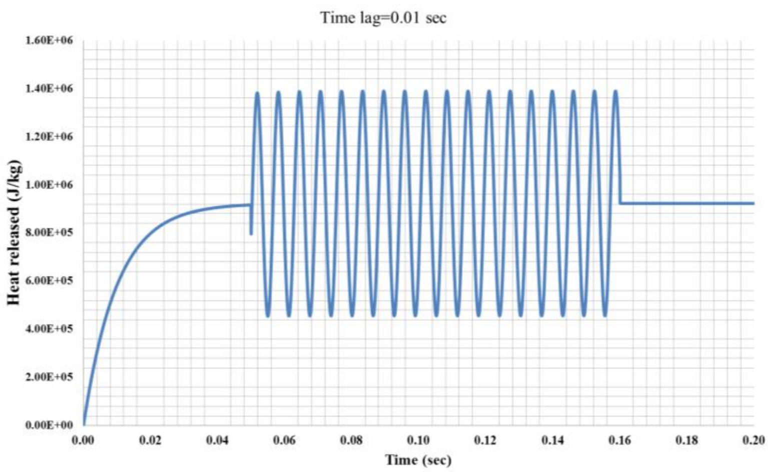

Figure 6. Specific heat released rate distribution.

Grid study

We perform some CFD simulations with different mesh sizes to study the independency of the solution. Here, the numbers of grids are 50, 100, 500, 1000 and 5000 respectively. Finally, a grid, which represents a suitable precision and computational cost, was selected. In this work, one-dimensional reacting compressible flow in a combustor is modeled. Figure 7 depicts the combustor outlet temperature, for each grid.

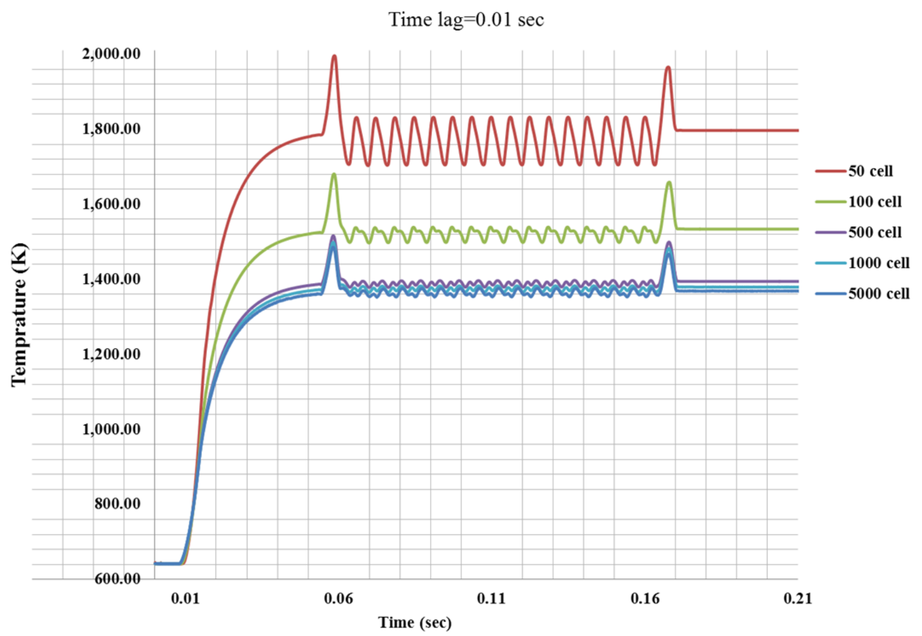

Figure 7. Combustor outlet temperature for different grid resolutions.

According to figure 7, it is observed that by increasing the number of cells, the temperature distribution throughout the chamber will converge to a steady-state. Also, it can be seen that through the convergence, the outlet temperature decreases. For example, with an increase in resolution of the computational grid from 50 to 500 cells, it is observed that the outlet temperature would decrease about 400 degrees. This is because of the numerical diffusion creation in the domain. Since the reduction of cell numbers, causes greater numerical diffusion in the flow field, higher numerical diffusion also results in energy transfer mechanism through diffusion as well as convection. Thus, in figure 7 the computational domain with fewer cells (higher numerical diffusion), will show greater outlet temperature. Finally, according to figure 7, it is observed that the temperature is almost constant by any further increase in cell number greater than 500 cells. Thus to obtain independent results from the computational grid, 500 cells is offered (Δx=0.002m).

Effects of fuel flow rate fluctuations on combustor outlet temperature

One of the key parameters for temperature distribution in the combustion chamber is fuel mass flow. In this section, we will take into account the fuel mass flow oscillation and its impact on outlet temperature. In figure 8, the effects of an increase in the oscillation of frequency, on the combustor outlet temperature, for low frequencies of 5, 10, 15 and 25 Hz are shown. By frequency raise, the maximum temperature increases. For frequencies less than 15 Hz, there is no fluctuation in temperature results. By the increase in frequency more than 15 Hz up to 25 Hz, the temperature will be oscillatory through the time, which its amplitude is being greater since the frequency increased.

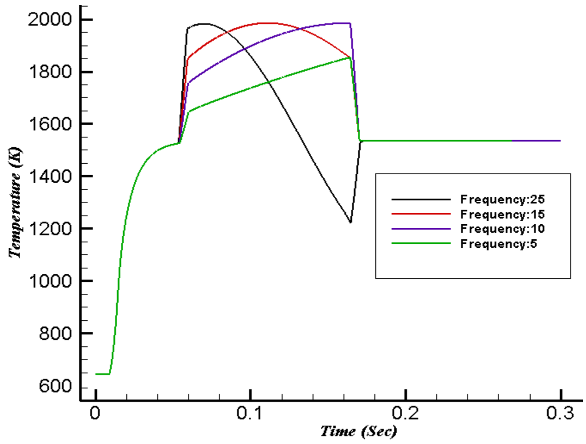

Figure 8. Combustor outlet temperature distribution variation for fuel flow rate fluctuations with frequencies, of 5, 10, 15 and 25 Hz.

Now, by increasing frequency, the oscillations are expected to be more intense therefore, the same model is applied for higher frequencies and results are presented in figure 9.

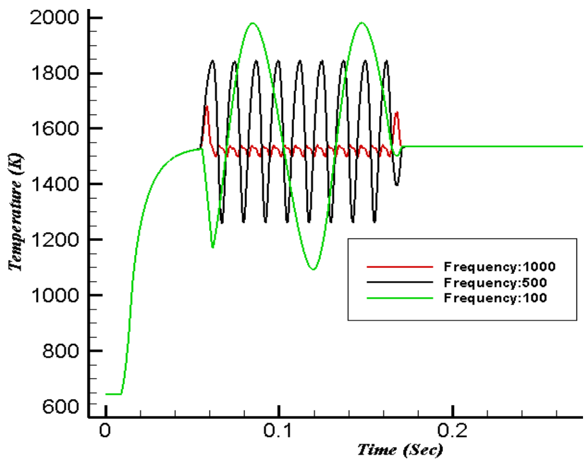

Figure 9. Combustor outlet temperature distribution variation for fuel flow rate fluctuations with frequencies of 100, 500 and 1000 Hz.

In figure 9, the effects of inlet frequency of oscillation, on the combustor outlet temperature variation, for higher frequencies of 100, 500 and 1000 Hz are shown. According to this figure the interval where fluctuations in temperature exist, (time between 0.5s to 0.15s); by increasing in frequency, the created fluctuations would decrease. Also, it can be seen, the amplitude of these oscillations by increasing in frequency would decrease. So that in the frequency of 1000 Hz, the amplitude of these fluctuations would decline intensely. It is perceived that enhancing the oscillation of amplitude increases the frequency up to 25 Hz. The amplitude would be constant in a range of 25 Hz up to 100 Hz and decreases for the frequency values, more than 100 Hz.

Effects of air flow rate fluctuations on combustor outlet temperature

In this section, the effect of air flow rate fluctuations on the performance of the combustion compared to the effect of fuel flow rate would be investigated. Therefore, boundary conditions, inputs, and assumptions are similar to the previous section. For the incoming air flow rate into the combustor in the dynamic model is considered and thus, the results on the outlet temperature of the combustion chamber will be discussed.

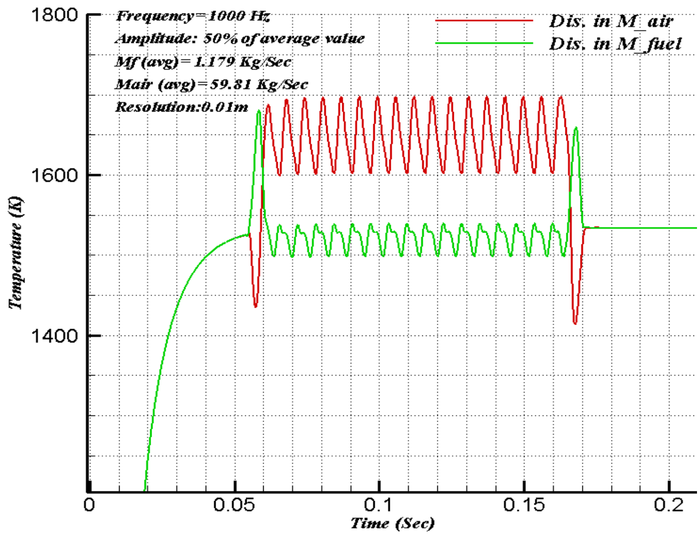

Figure 10. Combustor outlet temperature distribution variations with dynamic input of air mass flow rate.

Figure 10 shows the combustor outlet temperature variation versus time, to illustrate the effect of fluctuations on inlet fuel and air flow rate. It is observed that when the fuel flow rate is oscillating dynamically (in a specific time range t=0.05s to t=0.15s), the fluctuations of air flow rate has a similar effect in this interval. One of the most important results is the greater temperature of the outlet when the air mass flow fluctuates rather than fuel mass flow fluctuations. Also, it has been observed that the oscillation of amplitude for the air case is more than fuel.

Conclusion

The dynamic behavior of a gas turbine combustor is studied using high grid resolution numerical simulation of 1D Euler equations. A Eulerian-Lagrangian method is utilized to solve the governing equations. The effects of oscillations in the air and fuel mass flow rate on the outlet temperature of the chamber are then examined. The combustor flammability limits are determined by using experimental data and Le Chatelier's law. The main computing model constructed in Lagrangian coordinates via PPMLR algorithm which remaps the results to Eulerian coordinates, at the end of each time step. The model has validated with an analytical solution of a constant area combustion chamber. A comparison to the available analytical data is favorable. Also, the survey of grid resolution, which is varied in cell numbers from 50 to 500 cells, showed 400 degrees of increase in temperature. Then air and fuel mass flow oscillations have implemented to the combustor model to analyze its effects on combustor outlet temperature. In this case, the amplitude of temperature oscillations is studied. It is observed the increase in temperature oscillation of amplitude by an increase in the frequency of fuel flow up to 25 Hz. The amplitude would be constant in a range of 25 Hz up to 100 Hz and decreases for the frequency values, more than 100 Hz. Als, air mass flow fluctuations is studied and revealed that air mass flow fluctuations lead to more temperature than fuel oscillations. Additionally, the temperature oscillations amplitude is higher on the air fluctuations, than the fuel fluctuations.

Nomenclature

C	Sound speed
Cp	Specific heat ratio in constant pressure
E	Total energy
F	Momentum source term
f	Frequency
G	Energy source term
p	Pressure
Q	Heat released
t	Time
T	Temperature
u	Velocity
x	Horizontal coordinate
y	Vertical coordinate
ε	Specific energy
ρ	density
γ	Specific heat ratio
φ	Equivalence ratio

Subscripts

f	fuel
i	Entrance parameter
Pz	Primary zone of the combustion chamber
Mix	mixture

Reference

[1] Rodriguez, C.G., "One-dimensional finite-rate model for gas-turbine combustors", Ph.D. Thesis, Virginia Polytechnic Institute and State University (1997).

[2] Hale, A.A., and Davis, M.W., "Dynamic Turbine Engine Compressor Code DYNTECC - Theory and Capabilities", AIAA, 92-3190 (1992).

[3] Garrard, G.D., Davis, M.W. Jr., and A.A. Hale, "Recent Advances in Gas Turbine Engine Dynamic Models Developed Through JDAPS", ASME, 95-GT-146 (1995).

[4] Lefebvre, A.W., Gas Turbine Combustion, McGraw-Hill, 1983, p. 167.

[5] Navai, A., & Zamani Meymian, N. (2019, July 17). A Novel Method for Developing Compressor's Characteristic Curves Due to the Guide Vane Stagger Angle Variation. https://doi.org/10.31224/osf.io/d2ype.

[6] Zamani Meymian, N., & Khodadadi, R. (2019, July 19). One-Dimensional Numerical Analysis of Cross-Sectional Area Variation Effects on Flow through the Gas Turbine Diffuser. https://doi.org/10.31224/osf.io/ue47z.

[7] Gupta, A.K., and Lilley, D.G., "Combustion and Environmental Challenges for Gas Turbines in the 1990's", Journal of Propulsion and Power, 10: 137-147 (1994).

[8] Przybylko, S.J., “Application of System Identification Techniques to Post stall Combustor Dynamics”, AIAA. 85- 1353 (1985).

[9] Costura, D. M., Lawless, P. B., and Fankel, S. H., “A Computational Model for the Study of Gas Turbine Combustor Dynamics”. J. Eng. for Gas Turbines and Power. 121: No. 98-GT-342 (1999.).

[10] Colella, P. and Woodward, P. R., “The Piecewise Parabolic Method (PPM) for Gas-Dynamical Simulations”, J. Comput. Physics, 54: 174-201 (1984.).

[11] Khodadadi, R., & Zamani Meymian, N. (2019, July 25). Investigation of Influencing Parameters and Determination of the Lower and Upper Limits of Flammability of a 25MW Industrial Gas Turbine Combustor. https://doi.org/10.31224/osf.io/k937j.

[12] Zhao, F., “Experimental measurements and modeling prediction of flammability limits of binary hydrocarbon mixtures”, A Master of Science thesis submitted in Texas A&M University (2008).

[13] Emmons, H. W., Pearson, C. E., and Grant, H. P., “Compressor Surge and Stall Propagation”. ASME Transactions. 27: 455-469 (1955).

[14] Vanleer, B., “Towards the Ultimate Conservative Difference Scheme, a Second Order Sequel to Godunov's Method”. J. Comput. Physics. 32: 101-106 (1979).

[15] Hill, P.G., and Peterson, C.R., Mechanics, and Thermodynamics of Propulsion, 2nd Edition, Addison-Wesley Publishing Co. 1992.

[16] Shapiro, A., The Dynamics, and Thermodynamics of Fluid Flow, Ronald Press Co. 1952.